

AD-A134 683

SAMPLING MISMATCH AND TIMING JITTER IN PULSE-DOPPLER  
RADAR(U) MASSACHUSETTS INST OF TECH LEXINGTON LINCOLN  
LAB S C POHLIG 09 SEP 83 TR-646 ESD-TR-83-042  
F19628-80-C-0002

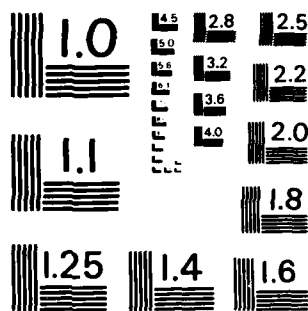
1/1

UNCLASSIFIED

F/G 17/9

NL

END  
DATE  
FILMED  
12 OCT  
DTIC



MICROCOPY RESOLUTION TEST CHART  
NATIONAL BUREAU OF STANDARDS-1963-A

12



MASSACHUSETTS INSTITUTE OF TECHNOLOGY  
LINCOLN LABORATORY

**SAMPLING MISMATCH AND TIMING JITTER  
IN PULSE-DOPPLER RADAR**

*S.C. POHLIG*

*Group 27*

TECHNICAL REPORT 646

9 SEPTEMBER 1983

Approved for public release; distribution unlimited.

LEXINGTON

MASSACHUSETTS

# ABSTRACT

Pulse-Doppler processing is an often used technique for extracting range and Doppler information of targets. Such a system can be described as consisting of three basic components, a pulse compressor, sampler, and Doppler processor. When quadrature detection is used, the gains and timing of the sampled inphase and quadrature components of the pulse compressor output must be matched in order to minimize distortion and noise at the Doppler processor output. In addition, the jitter in the sampling times also causes distortion and noise. This report presents an analysis of these effects and describes the signal degradations due to mismatch and jitter in the sampler.

Accession For	
NTIS GRA&I	<input checked="" type="checkbox"/>
DTIC TAB	<input type="checkbox"/>
Unannounced	<input type="checkbox"/>
Justification	
By	
Distribution/	
Availability Codes	
Dist	Avail and/or Special
A-1	



## TABLE OF CONTENTS

	<u>Page</u>
Abstract	iii
List of Figures	vii
1. INTRODUCTION	1
2. GAIN MISMATCH	7
3. SAMPLING TIME MISMATCH	11
4. TIMING JITTER	15
4.1 Clock Frequency Jitter	15
4.2 Independent Random Jitter	22
4.3 Combined Jitter Model	28
5. CONCLUSION	30
Acknowledgements	31
References	32
Appendix A	33

## LIST OF FIGURES

	<u>Page</u>
1. LFM Burst Waveform	2
2. Pulse Compressed Waveform	2
3. Pulse-Doppler Processor	2
4. False Target Level for Gain Mismatch	9
5. SNR Loss for Gain Mismatch	9
6. False Target Level for Timing Mismatch	14
7. SNR Loss for Timing Mismatch	14
8. Distortion Level for Clock Frequency Jitter	23
9. Distortion Level for Independent Random Jitter	26
10. Relative Average Distortion at Doppler Peak	26



## 1. INTRODUCTION

Pulse-Doppler processing is used to obtain range and velocity information of targets for radar applications such as ballistic missile defense. A radar system based on this type of processing transmits a waveform which consists of a sequence of pulses uniformly spaced in time. Each of these pulses is linear frequency modulated (LFM) and is identical to the other pulses (except possibly for a weighting factor). The components of this waveform are shown in Figure 1.

The received waveform (for a single target) is very similar to that shown in Figure 1, except that the signal is delayed in time corresponding to the target range, and the signal is Doppler shifted in frequency corresponding to target velocity. In addition, noise is added to the signal. The received signal is first filtered by a pulse compressor (matched filter for a LFM pulse), producing the signal shown in Figure 2. This pulse compressed signal is converted from a continuous signal to a sampled data set by a sampler, and the sampled data is then processed by a Doppler processor. For a given range cell, the Doppler processor computes the discrete Fourier transform (DFT) of a set of samples which are spaced in time by an amount equal to the pulse spacing shown in Figures 1 and 2. The number of points used in the DFT is equal to the number of pulses in the waveform. The Doppler shift of the target is proportional to the rate of change of phase from sample to sample, and appears in the DFT output as a peak at the Doppler frequency. Figure 3 shows a simplified diagram of a pulse-Doppler processor.

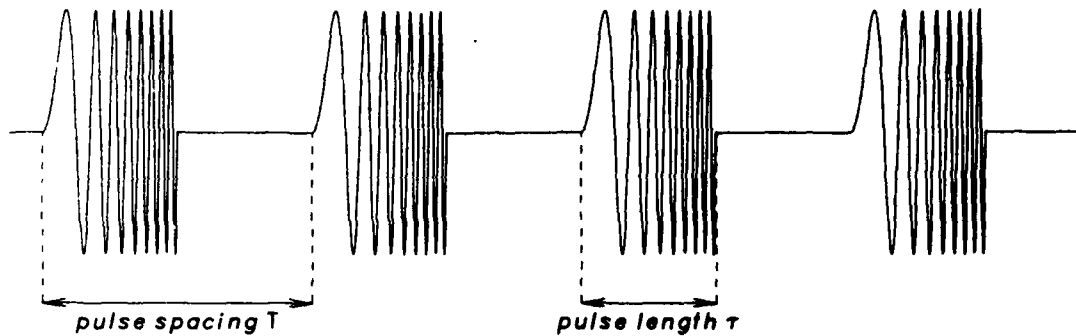


Figure 1. LFM Burst Waveform

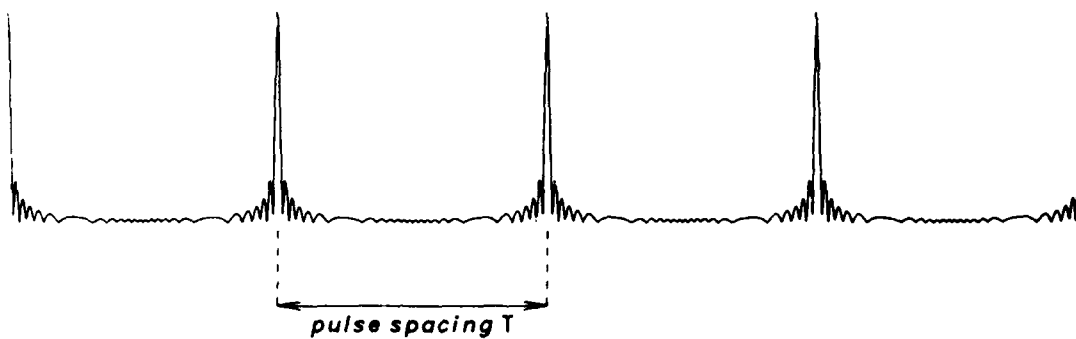


Figure 2. Pulse Compressed Waveform

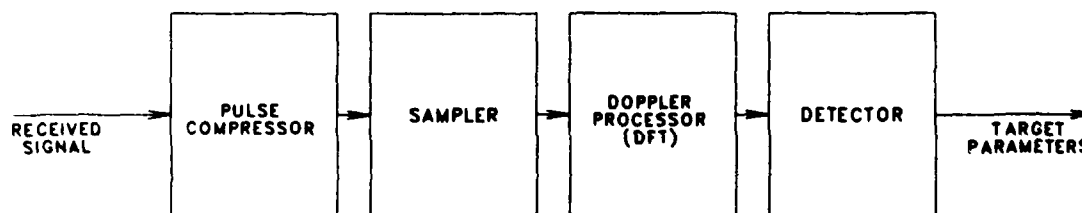


Figure 3. Pulse-Doppler Processor

One of the limitations in the system just described is that the sampler is not perfect, but instead exhibits a certain amount of mismatch between the gains and sampling times of the inphase and quadrature (I and Q, real and imaginary) components of the sampled pulse compressed signal. The sampling times are also subject to random jitter. These nonideal characteristics cause noise and distortion to appear in the DFT output, so that target detection becomes more difficult.

The purpose of this paper is to describe analytically the degradation of pulse-Doppler processing due to sampler imperfections. This analysis requires an understanding of the signal being sampled, the pulse compressed waveform shown in Figure 2. This waveform can be described in terms of the time-frequency autocorrelation function.

The time-frequency autocorrelation  $\chi(t,f)$  of a signal  $p(t)$  is obtained by convolving a frequency shifted and time shifted version of  $p(t)$  with a matched filter for  $p(t)$ . From Nathanson [1, p. 284],

$$\chi(t,f) = \int_{-\infty}^{\infty} p(u)p^*(u+t)e^{-j2\pi fu} du \quad .$$

For example, the formula of a LFM pulse [1, pp. 287-288] is

$$p(t) = \exp[j2\pi(f_0 t + kt^2/2)], \quad |t| \leq \tau/2 \quad (1)$$

for pulse length  $\tau$  and bandwidth  $k\tau$ , and the corresponding function  $\chi(t,f)$  is

$$\chi(t,f) = e^{j\pi ft} \frac{\sin[\pi(kt+f)(\tau-|t|)]}{\pi(kt+f)\tau} \quad , \quad |t| \leq \tau \quad . \quad (2)$$

Note that in Equation (2),  $\chi(t,f) = \chi(-t,-f)$ . The nature of  $\chi(t,f)$  is that

there is a peak at  $t = -f/k$  with nominal width  $1/k\tau$ . Away from the peak,  $\chi(t,f)$  diminishes, and is identically zero for  $|y| > \tau$ . The purpose of pulse compression is to obtain a width  $1/k\tau$  which is much less than  $\tau$ . The narrowing of the width yields improved range resolution.

The transmitted radar waveform is a sequence  $s(t)$  of LFM pulses

$$s(t) = \sum_{m=0}^{N-1} p(t-mT) \quad (3)$$

where  $T \geq \tau$  is the pulse spacing indicated in Figure 1. The received radar signal  $r(t)$  is a Doppler-shifted and time-delayed version of  $s(t)$ .

$$r(t) = s(t-\rho)e^{j2\pi ft}$$

Letting  $p^*(-t)$  be the pulse compressor, the pulse compressed waveform is obtained by filtering  $r(t)$  with  $p^*(-t)$ . The result is

$$y(t) = \sum_{m=0}^{N-1} \chi(t-mT-\rho, f)e^{j2\pi fmT} + n(t) \quad (4)$$

where  $n(t)$  is a random noise signal,  $\rho$  is the delay due to range, and  $f$  is the Doppler shift. For simplicity, we are assuming a target signal amplitude of unity. In a pulse-Doppler radar, the width of the peak in  $\chi(t,f)$  is much less than  $\tau$  and thus much less than  $T$ . Thus, we can make an approximation for  $y(t)$  in the vicinity of the peaks,

$$y(t) = \chi(t-mT-\rho, f)e^{j2\pi fmT} + n(t) \quad (5)$$

for

$$(mT+\rho-f/k) - 1/2k\tau \leq t \leq (mT+\rho-f/k) + 1/2k\tau$$

This approximation is actually an equality when  $T > \tau + 1/2k\tau$  since  $\chi(t, f)$  is zero for  $|t| > \tau$ . For an N pulse waveform, Doppler processing is performed by computing the DFT of N samples of  $y(t)$  uniformly spaced with spacing T. If we let the m-th sample occur at  $t_m = t' - f/k + mT + p$  where  $|t'| < 1/2k\tau$ , then the DFT input samples are

$$x_m = \chi(t' - f/k, f) e^{j2\pi f m T} + n(t_m), \quad m=0, \dots, N-1 \quad (6)$$

and each of the samples occurs within the peak of  $\chi$ . This definition of  $t'$  corresponds to examining the range cell in which the target is, where  $t'$  is the distance from the center of the range cell. The analysis in the following sections is made easier by writing  $x_m$  in terms of the real-valued function  $G(t, f)$ ,

$$\begin{aligned} G(t, f) &= \chi(t, f) e^{-j\pi f t} \\ &= \frac{\sin[\pi(kt+f)(\tau - |t|)]}{\pi(kt+f)\tau} \end{aligned} \quad (7)$$

From Equations (6) and (7), we have

$$x_m = G(t' - f/k, f) e^{j2\pi f m T + j\theta} + n(t_m) \quad (8)$$

where  $\theta = \pi f(t' - f/k)$  and does not depend on m. Note that the samples in Equation (8) are of a noisy sinusoid, where the sinusoid component is multiplied by a term which is independent of the sample index m. Thus, the DFT of  $x_0, \dots, x_{N-1}$  is the DFT of a noisy sinusoid. The location of the peak in the DFT output depends on f and T, and indicates the amount of Doppler shift.

In the following sections, Equation (8) will be used to determine the effects of sampling gain mismatch, timing mismatch, and timing jitter. Section 2 investigates gain mismatch, Section 3 examines sample time mismatch, and Section 4 discusses the effects of sample timing jitter.

## 2. GAIN MISMATCH

This section examines the effect of mismatched I and Q gains on the sampling process. It will be shown that the result is the appearance of a false target, plus reduced SNR.

If we let  $a$  and  $b$  be the gains of the I and Q components of the sampler, then the samples of Equation (8) become

$$x_m = [a \cos(2\pi f_m T + \theta) + jb \sin(2\pi f_m T + \theta)]G(t' - f/k, f) + an_I(m) + jbn_Q(m) \quad (9)$$

where  $n_I(m)$  and  $n_Q(m)$  are the I and Q components of the noise. The form of  $x_m$  can be arranged to show the resulting degradations without having to compute the DFT of these samples. Equation (10) shows that  $x_m$  is equivalent to samples of a signal which consists of two targets plus noise, where the targets are at the same range, but with opposite Doppler shifts.

$$x_m = \left[ \frac{a+b}{2} e^{j2\pi f_m T + j\theta} + \frac{a-b}{2} e^{-j2\pi f_m T - j\theta} \right] G(t' - f/k, f) + an_I(m) + jbn_Q(m) \quad (10)$$

The first term in Equation (10) corresponds to the true target, and the second term is a false target. The ratio of the false target signal power to the true target signal power (FTR) is easily computed as the ratio of the square of the relative amplitudes.

$$\text{FTR} = \left( \frac{a-b}{a+b} \right)^2 \quad (11)$$

The relative strength of the false target is shown in Figure 4 as a function of the ratio of I and Q gains.

The loss in signal-to-noise ratio (SNR) due to gain mismatch can also be easily determined. If the noise samples  $n_I(m)$  and  $n_Q(m)$  are independent and have equal variances (power), then the noise power is multiplied by the factor

$$\frac{a^2 + b^2}{2g^2} \quad (12)$$

where  $g$  is the ideal gain. Similarly, the signal power is multiplied by the factor

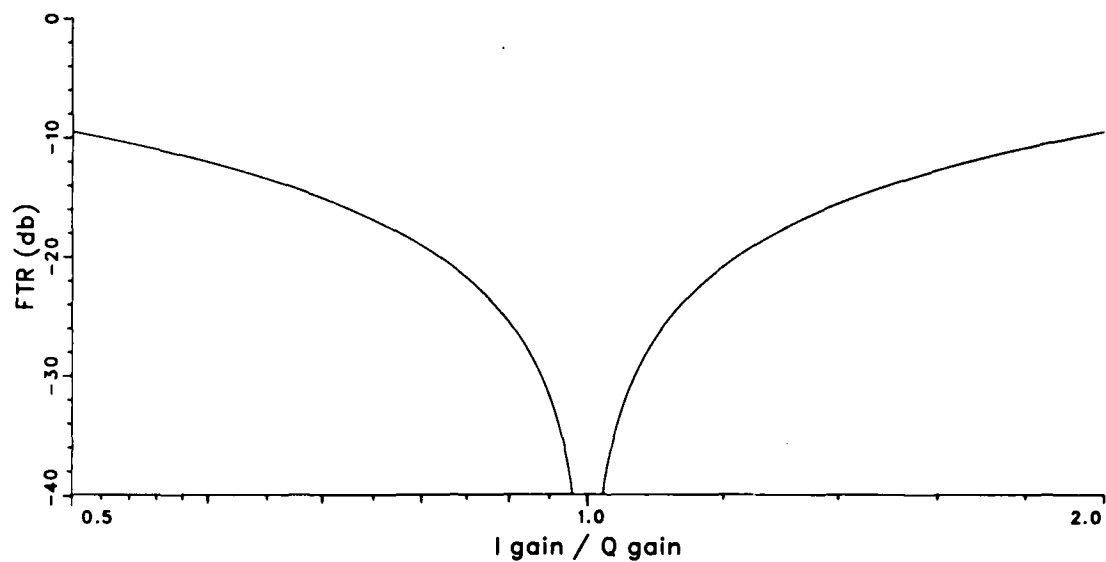
$$\frac{(a+b)^2}{4g^2} \quad (13)$$

The ratio of these two functions gives the ratio between the mismatched SNR and the matched SNR, which is a net loss. This loss in db is

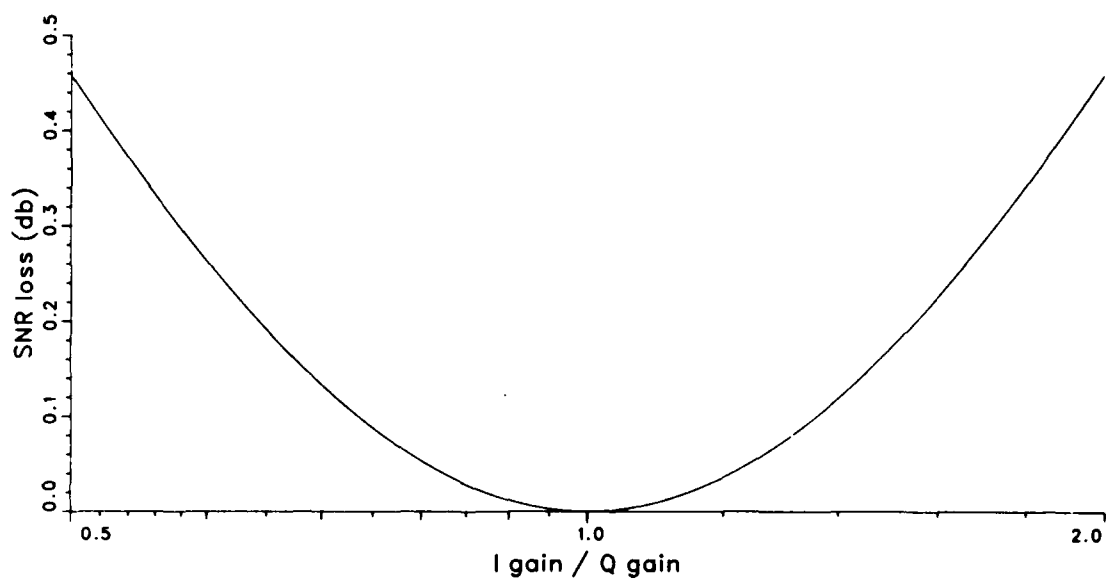
$$\text{LOSS} = 10 \log \frac{2(a^2 + b^2)}{(a+b)^2} \quad (14)$$

Figure 5 shows the loss as a function of gain mismatch. It is seen that the loss is not large for reasonable amounts of mismatch. The next section





**Figure 4. False Target Level for Gain Mismatch**



**Figure 5. SNR Loss for Gain Mismatch**

discusses the effects of timing mismatch. It will be shown that timing mismatch can be related to a target dependent form of gain mismatch, again resulting in a false target and SNR loss.

### 3. SAMPLING TIME MISMATCH

In this section, we investigate the result of timing mismatch between the I and Q samples. As in the previous section, the analysis will be restricted to a single target in the presence of noise. The results carry over to multiple targets.

To investigate the effects of timing mismatch, we modify Equation (8) so that the I component is sampled at time  $t_m + \delta$  and the Q component is sampled at time  $t_m - \delta$  where

$$t_m = t' - f/k + mT + p \quad (15)$$

is the nominal sampling time for the  $m$ -th sample. In this case, the samples are

$$\begin{aligned} x_m = & \cos[2\pi f(mT + \delta) + \theta] G(t' - f/k + \delta, f) \\ & + j \sin[2\pi f(mT - \delta) + \theta] G(t' - f/k - \delta, f) \\ & + n_I(m) + j n_Q(m) \end{aligned} \quad (16)$$

where  $n_I$  and  $n_Q$  are the time-shifted noise terms. If the two noise terms are independent and represent a stationary random process, then the noise power and statistics are independent of  $\delta$ . In Appendix A, it is shown that the effect of  $\delta$  in the sin and cos functions of Equation (16) is much less significant than that of  $\delta$  in the function  $G$ , and that the  $\delta$  in the sin and cos can be dropped.

As in Section 2, the expression for the samples can be arranged to appear as two targets plus noise:

$$\begin{aligned}
 x_m = & \frac{1}{2} [G(t'-f/k+\delta, f) + G(t'-f/k-\delta, f)] e^{j2\pi f m T + j\theta} \\
 & + \frac{1}{2} [G(t'-f/k+\delta, f) - G(t'-f/k-\delta, f)] e^{-j2\pi f m T - j\theta} \\
 & + n_I(m) + j n_Q(m) \quad . \quad (17)
 \end{aligned}$$

The first term corresponds to the true target and the second term corresponds to a false target at the same range, but with the opposite Doppler shift. The ratio of false target power to true target power is

$$FTR = \frac{[G(t'-f/k+\delta, f) - G(t'-f/k-\delta, f)]^2}{[G(t'-f/k+\delta, f) + G(t'-f/k-\delta, f)]^2} \quad . \quad (18)$$

Since the noise power is unaffected by timing mismatch, the loss in SNR is equal to the loss in signal power. In db relative to the no mismatch case, this loss is

$$LOSS = 10 \log \frac{4G(t'-f/k, f)^2}{[G(t'-f/k+\delta, f) + G(t'-f/k-\delta, f)]^2} \quad . \quad (19)$$

Notice that both the FTR and the SNR loss depend strongly on the target range and Doppler shift. Figure 6 shows the FTR as a function of the mismatch  $2\delta$  (expressed as a fraction of the Nyquist sampling interval  $1/k\tau$ ) for the case where the bandwidth,  $k\tau$ , is much greater than the Doppler shift,  $f$ , and where the pulse length,  $\tau$ , is much longer than the sampling interval,  $1/k\tau$ . The worst case is obtained when the peak of the response is located between two

range cells (i.e., the peak is located 1/2 sampling period from where the sample is actually taken). With Nyquist sampling, the sampling period is  $1/k\tau$  and the worst case occurs when  $t' = \pm 1/2k\tau$ . The derivation is not given here, but it can be shown that the worst case is approximately  $20 \log(2\delta k\tau)$ . The average case is obtained by averaging the FTR for target peaks located from 1/2 sampling period before the nominal sampling point to 1/2 period after. It is interesting to note that the average is a constant 6 db better than the worst case. Figure 7 shows the SNR loss for the example of Figure 6.

The above analysis can easily be adapted to include both gain and timing mismatch. In this case, we have

$$\text{FTR} = \frac{[aG(t'-f/k+\delta, f) - bG(t'-f/k-\delta, f)]^2}{[aG(t'-f/k+\delta, f) + bG(t'-f/k-\delta, f)]^2} \quad (20)$$

and

$$\text{LOSS} = 10 \log \frac{2(a^2+b^2)G(t'-f/k, f)^2}{[aG(t'-f/k+\delta, f) + bG(t'-f/k-\delta, f)]^2} \quad (21)$$

Thus far, we have seen that both gain mismatch and timing mismatch lead to false targets and reduced SNR. The next section examines the effects due to timing jitter. It will be seen that jitter causes additional target dependent distortion.

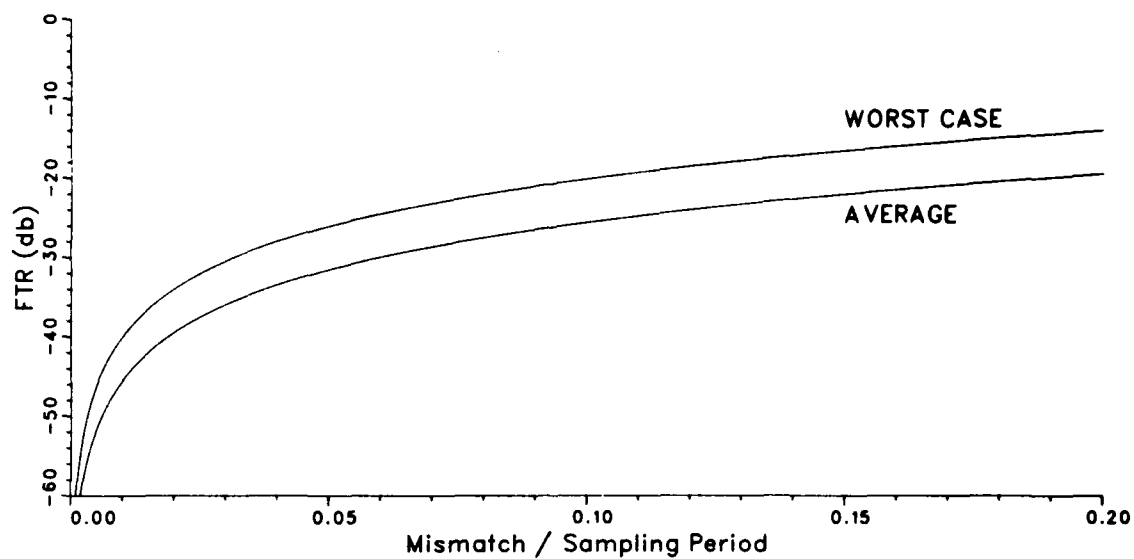


Figure 6. False Target Level for Timing Mismatch

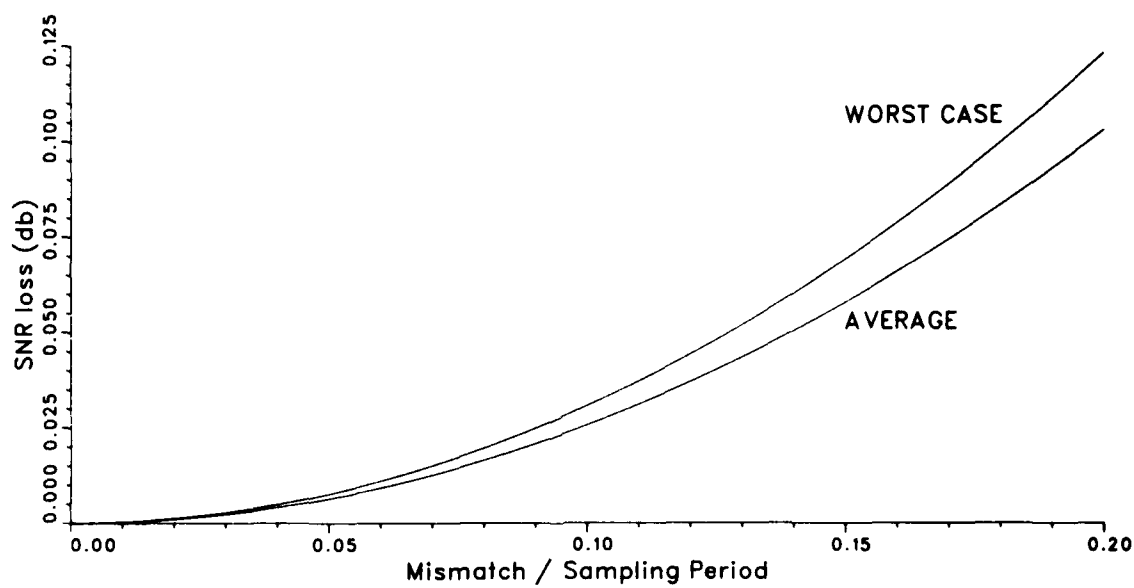


Figure 7. SNR Loss for Timing Mismatch

#### 4. TIMING JITTER

In this section, we examine the effects due to sampling time jitter. Two different models are considered for jitter. The case of frequency jitter in the system sampling clock is discussed first, and is followed by a discussion of independent random jitter. The final part of this section combines both jitter models.

##### 4.1 Clock Frequency Jitter

The samples in the case of sampling frequency jitter are modelled as sampling the I channel at time  $u_m = t_m + \delta + r_m$  with gain  $a$ , and the Q channel at time  $v_m = t_m - \delta + r_m$  with gain  $b$ . The terms  $a, b, \delta$  represent the gain and timing mismatch discussed in earlier sections. The  $r_m$  are a random process representing the jitter.

A good model of this jitter process is to represent the difference  $r_m - r_{m-1}$  as an independent Gaussian process with zero mean and variance  $\sigma^2$ . The justification for this model is that the system clock, which is used to drive the sampling process, can be represented as having a random clock period which is independent from one clock cycle to the next, and has a stationary mean. The system clock operates at a frequency greater than or equal to the sampling rate, which in turn is greater than or equal to the bandwidth,  $\kappa$ . The samples used for the Doppler processing of a given range cell, however, are spaced by the pulse spacing,  $T$ , as described in Section 1.

Since the pulse spacing is much greater than the sampling period, the pulse spacing is the sum of a large number of system clock periods. Since these clock periods are modelled as independent, identically distributed random variables, we have by the central limit theorem [2] that  $u_m - u_{m-1}$  and  $v_m - v_{m-1}$ , the time between two samples used for Doppler processing, are Gaussian distributed random variables, with mean  $T$ . (The variance of these random variables is defined as  $\sigma^2$ . Note that  $\sigma^2$  is the product of the variance of the system clock period and the number of clock periods which occur during time  $T$ . Thus,  $\sigma^2$  is proportional to  $T$ .) By the definition given above for  $u_m$  and  $v_m$ , we have that  $r_m - r_{m-1}$  is Gaussian with zero mean and variance  $\sigma^2$ .

As an example, consider the case of  $k\tau = 50$  MHz bandwidth, and  $T = 4 \mu\text{sec}$  pulse spacing. The number of system clock periods between two samples used for Doppler processing is at least  $k\tau T = 200$ .

Without loss of generality, we define  $\rho$ , the time delay due to target range, such that the jitter is zero at time  $(t_0 + t_{N-1})/2$ . (As in the previous sections, only the range cell which includes the target is analyzed.) Since  $u_m - u_{m-1}$  and  $v_m - v_{m-1}$  are Gaussian with mean  $T$  and variance  $\sigma^2$ , the definition of  $\rho$  implies that  $u_m - (u_0 + u_{N-1})/2$  and  $v_m - (v_0 + v_{N-1})/2$  are Gaussian with mean  $mT - T(N-1)/2$  and variance  $|m - (N-1)/2| \sigma^2$ . Thus,  $r_m$  is Gaussian with zero mean and variance  $|m - (N-1)/2| \sigma^2$ .

In order for the Doppler processing to be effective, it is necessary that the standard deviation of the jitter be less than the sampling interval. That is,  $\sigma \sqrt{(N-1)/2} < 1/k\tau$  for the extremes  $m=0$  and  $m=N-1$ .



Applying the above definitions to Equation (8) gives the following samples,

$$\begin{aligned}
 x_m = & aG(t'-f/k+r_m+\delta, f)\cos[2\pi fmT + \theta + \pi f(r_m+\delta)] \\
 & + jbG(t'-f/k+r_m-\delta, f)\sin[2\pi fmT + \theta + \pi f(r_m-\delta)] \\
 & + an_I(m) + jbn_Q(m)
 \end{aligned} \tag{22}$$

where  $\theta = \pi f(t'-f/k)$  and where  $n_I(m)$  and  $n_Q(m)$  are the noise components. Similar to the approximation made in the previous section, it is assumed that the sampling mismatch plus jitter is less than one sampling period. Since the sampling period is no greater than  $1/k\tau$ , we have  $|r_m \pm \delta| < 1/k\tau$ . Again, using the result given in Appendix A, we have that the arguments to the sine and cosine in Equation (22) are essentially  $2\pi fmT + \theta$ . The samples can now be written as

$$\begin{aligned}
 x_m = & aG(t'-f/k+r_m+\delta, f)\cos(2\pi fmT + \theta) + jbG(t'-f/k+r_m-\delta, f)\sin(2\pi fmT + \theta) \\
 & + an_I(m) + jbn_Q(m)
 \end{aligned} \tag{23}$$

These samples can be rewritten as the sum of a jitter-free signal and a jitter-dependent signal.

$$\begin{aligned}
 x_m = & aG(t'-f/k+\delta, f)\cos(2\pi fmT + \theta) + jbG(t'-f/k-\delta, f)\sin(2\pi fmT + \theta) \\
 & + a\alpha_m \cos(2\pi fmT + \theta) + jb\beta_m \sin(2\pi fmT + \theta) \\
 & + an_I(m) + jbn_Q(m)
 \end{aligned} \tag{24}$$

where the terms containing jitter are

$$\begin{aligned}\alpha_m &= G(t'-f/k+r_m+\delta, f) - G(t'-f/k+\delta, f) \\ \beta_m &= G(t'-f/k+r_m-\delta, f) - G(t'-f/k-\delta, f)\end{aligned}\quad (25)$$

From the analysis of the preceding section, we know that the jitter-free terms of Equation (24) lead to a false target and reduced SNR due to the gain and timing mismatch. The jitter-dependent terms in Equation (24) represent a random distortion. This distortion may be computed in order to determine the signal-to-distortion ratio (SDR) due to jitter.

The expected value of the distortion in the samples  $x_0, \dots, x_{N-1}$  is defined to be

$$D_1 = E \left[ \sum_{m=0}^{N-1} \left| a\alpha_m \cos(2\pi f_m T + \theta) + jb\beta_m \sin(2\pi f_m T + \theta) \right|^2 \right] \quad (26)$$

If we define the second moments of  $\alpha_m$  and  $\beta_m$  as

$$\begin{aligned}A_m &= E[\alpha_m^2] \\ B_m &= E[\beta_m^2]\end{aligned}\quad (27)$$

then the distortion,  $D_1$ , can be written as

$$D_1 = \sum_{m=0}^{N-1} [a^2 A_m \cos^2(2\pi f_m T + \theta) + b^2 B_m \sin^2(2\pi f_m T + \theta)] \quad (28)$$

Unfortunately, a closed-form solution for  $A_m$  and  $B_m$  is not available. In order to provide an understandable expression for  $D_1$ ,  $A_m$  and  $B_m$  may be computed by approximating  $\alpha_m$  and  $\beta_m$  with a second-order Taylor series about the point  $r=0$  [3]. Making the definitions

$$\begin{aligned} g_1 &= \frac{d}{dr} G(t' - f/k + r + \delta, f) \Big|_{r=0} \\ g_2 &= \frac{1}{2} \frac{d^2}{dr^2} G(t' - f/k + r + \delta, f) \Big|_{r=0} \\ h_1 &= \frac{d}{dr} G(t' - f/k + r - \delta, f) \Big|_{r=0} \\ h_2 &= \frac{1}{2} \frac{d^2}{dr^2} G(t' - f/k + r - \delta, f) \Big|_{r=0} \end{aligned} \quad (29)$$

gives the approximations

$$\begin{aligned} \alpha_m &\approx g_1 r_m + g_2 r_m^2 \\ \beta_m &\approx h_1 r_m + h_2 r_m^2 \end{aligned} \quad (30)$$

and since  $r_m$  is Gaussian with zero mean and variance  $|m-(N-1)/2|\sigma^2$ ,

$$\begin{aligned} A_m &\approx 3g_2^2\sigma^4(m-(N-1)/2)^2 + g_1^2\sigma^2|m-(N-1)/2| \\ B_m &\approx 3h_2^2\sigma^4(m-(N-1)/2)^2 + h_1^2\sigma^2|m-(N-1)/2| \end{aligned} \quad (31)$$

In the case of no gain or time delay mismatch ( $a=b$ ,  $\delta=0$ ), we have  $A_m=B_m$  and the distortion is

$$D_1 \approx \sum_{m=0}^{N-1} a^2 [3g_2^2\sigma^4(m-(N-1)/2)^2 + g_1^2\sigma^2|m-(N-1)/2|] \quad (32)$$

This formula reduces to

$$D_1 \approx \frac{1}{4} a^2 g_2^2 \sigma^4 (N^3 - N) + \frac{1}{4} a^2 g_1^2 \sigma^2 (N^2 - 1), \quad N \text{ odd} \quad (33)$$

$$D_1 \approx \frac{1}{4} a^2 g_2^2 \sigma^4 (N^3 - N) + \frac{1}{4} a^2 g_1^2 \sigma^2 N^2, \quad N \text{ even} \quad (34)$$

Note that  $g_1$  and  $g_2$ , and thus  $D_1$ , depend on target Doppler shift and range.

When mismatch is also present, the distortion,  $D_1$ , can be bounded by noting that  $\cos^2(t) \leq 1$  and  $\sin^2(t) \leq 1$ . The result is a formula similar to Equation (34),

$$D_1 \leq \frac{1}{4} \sigma^4 (a^2 g_2^2 + b^2 h_2^2) (N^3 - N) + \frac{1}{4} \sigma^2 (a^2 g_1^2 + b^2 h_1^2) N^2 \quad (35)$$

In the case of no mismatch, the upperbound in Equation (35) is two times the formula in Equation (34).

At this point all that remains in computing the SDR is to compute the signal power. Applying the discussion in Section 3 to the samples in Equation (24), the amplitude of the true target is

$$\frac{1}{2} [aG(t' - f/k + \delta, f) + bG(t' - f/k - \delta, f)] \quad (36)$$

The signal power in samples  $x_0, \dots, x_{N-1}$  is then

$$\begin{aligned} S &= \sum_{m=0}^{N-1} \frac{1}{4} [aG(t' - f/k + \delta, f) + bG(t' - f/k - \delta, f)]^2 \\ &= \frac{N}{4} [aG(t' - f/k + \delta, f) + bG(t' - f/k - \delta, f)]^2 \end{aligned} \quad (37)$$

In the case of no gain or time delay mismatch, the signal power is

$$S = N a^2 G^2(t' - f/k, f) \quad (38)$$

Defining  $SDR_1$  as  $S/D_1$  and using the above equations for  $S$  and  $D_1$ , it is apparent that for a fixed pulse spacing, the  $SDR_1$  prior to Doppler processing is inversely proportional to  $N^2$ , the square of the number of pulses in the burst. Since, as mentioned earlier,  $\sigma^2$  is proportional to the pulse spacing,

$T$ , the SDR is inversely proportional to  $T^2$  also. These comments may be combined to show that the  $SDR_1$  is inversely proportional to the square of the length of the pulse compressed waveform,  $(N-1)^2 T^2$ .

As an example of the SDR, consider the case where the bandwidth,  $k\tau$ , is much greater than the Doppler shift,  $f$ , and the pulse length,  $\tau$ , is much greater than the sampling period,  $1/k\tau$ . Figure 8 shows the SDR (averaged over target range) defined by Equations (34) and (38). This curve is shown as a function of  $N$ , the number of pulses in the waveform, and as a function of the amount of jitter,  $\sigma$ , for a  $N=16$  pulse waveform.

#### 4.2 Independent Random Jitter

The samples in the case of independent random jitter are obtained by sampling the I channel at time  $t_m + \delta + r_m$  with gain  $a$ , and the Q channel at time  $t_m - \delta + s_m$  with gain  $b$ . As in earlier discussions,  $a, b, \delta$  represent gain and time delay mismatch. The  $r_m$  and  $s_m$  are independent and identically distributed random variables representing the timing jitter, and are modelled as having zero mean and variance  $\gamma^2$ .

The justification of this independent random jitter model is that jitter can be observed in electronic systems, even though the system clock is stable during the observation time. For example, in digital systems, noise (e.g., crosstalk or thermal noise) can combine with the nonzero rise and fall times of logic signals to cause logic circuits to change states at a somewhat random time with respect to the ideal time of the state change.

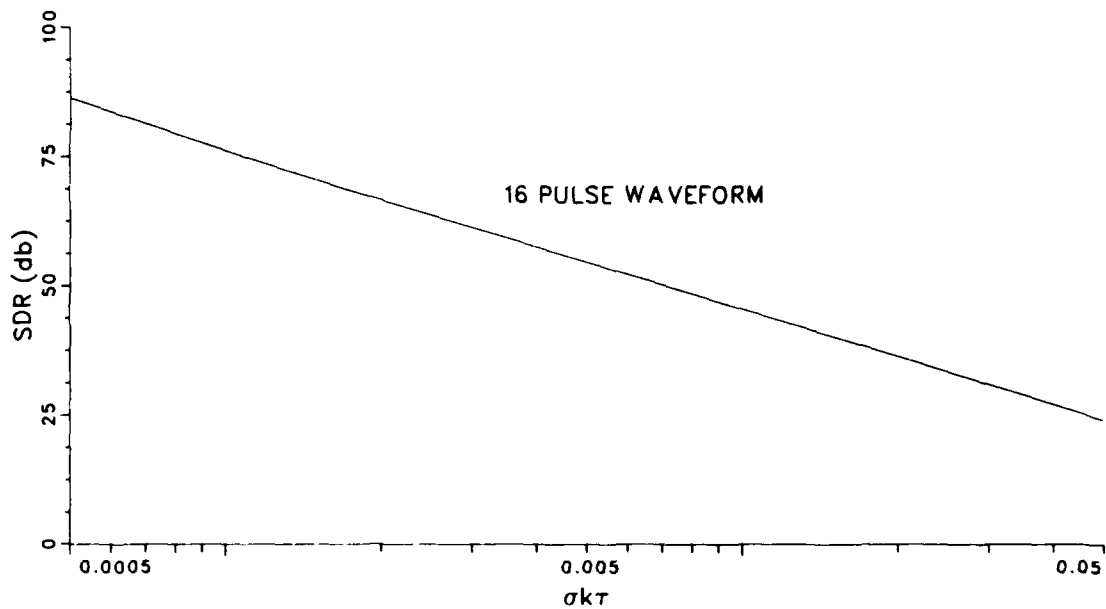
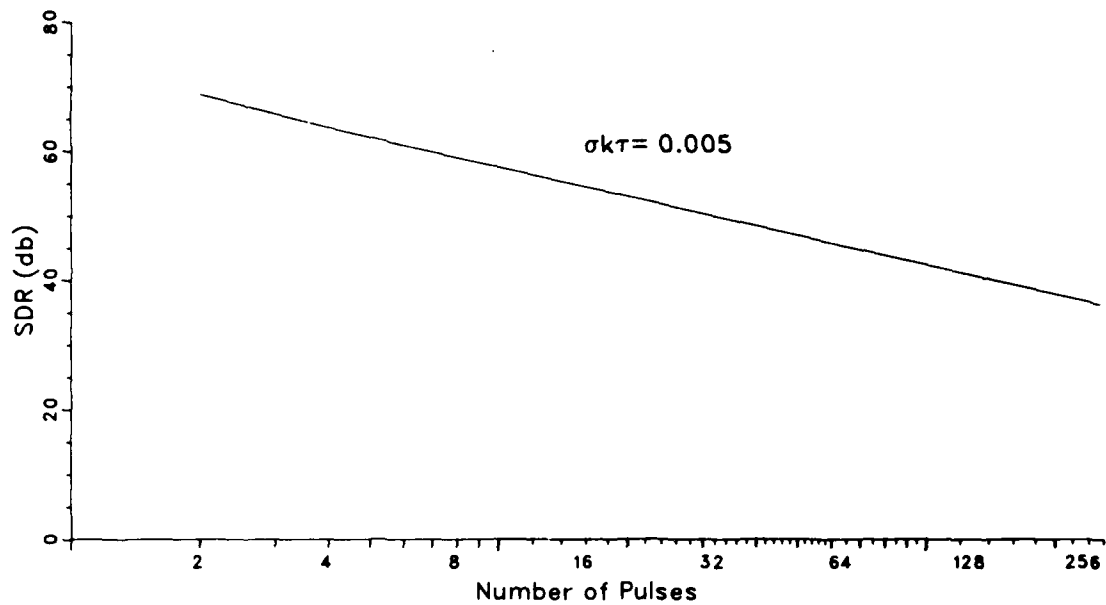


Figure 8. Distortion Level for Clock Frequency Jitter

The analysis of this random jitter case parallels the analysis in Section 4.1, producing a false target, reduced SNR, and target dependent distortion. The result similar to Equation (28) is that the distortion,  $D_2$ , is

$$D_2 = \sum_{m=0}^{N-1} [a^2 \cos^2(2\pi f_m T + \theta) E[\alpha_m^2] + b^2 \sin^2(2\pi f_m T + \theta) E[\beta_m^2]] \quad (39)$$

where

$$\begin{aligned} \alpha_m &= G(t' - f/k + r_m + \delta, f) - G(t' - f/k + \delta, f) \\ \beta_m &= G(t' - f/k + s_m - \delta, f) - G(t' - f/k - \delta, f) \end{aligned} \quad (40)$$

Using a second-order Taylor series as before, and modelling  $r_m$  and  $s_m$  as independent, identically distributed random variables with zero mean and a symmetric density function gives the approximations

$$\begin{aligned} E[\alpha_m^2] &\approx 3g_2^2 \gamma^4 + g_1^2 \gamma^2 \\ E[\beta_m^2] &\approx 3h_2^2 \gamma^4 + h_1^2 \gamma^2 \end{aligned} \quad (41)$$

where  $g_1, g_2, h_1, h_2$  are defined in Equation (29). Applying Equation (41) to



Equation (39) and assuming no gain or delay mismatch gives

$$D_2 = a^2 N (3g_2^2 \gamma^4 + g_1^2 \gamma^2) \quad . \quad (42)$$

When mismatch is present, a bound on the distortion can be given as

$$D_2 \leq a^2 N (3g_2^2 \gamma^4 + g_1^2 \gamma^2) + b^2 N (3h_2^2 \gamma^4 + h_1^2 \gamma^2) \quad . \quad (43)$$

The signal-to-distortion ratio,  $SDR_2 = S/D_2$ , is computed by using the formula for  $S$  in Equation (37) or (38) with Equation (42) or (43). Since both  $S$  and  $D_2$  are proportional to  $N$ , the ratio  $SDR_2$  does not depend on  $N$ . Note also that  $SDR_2$  does not depend on the pulse spacing,  $T$ . However,  $SDR_2$  does depend on target range and Doppler shift.

As an example, the  $SDR_2$  is plotted as a function of  $\gamma$  in Figure 9 for the same example used in Section 4.1 with Figure 8, assuming no gain or mismatch. As before,  $SDR_2$  is averaged over target range.

In the case of independent random jitter, it can be shown that the distortion component in the Doppler processor output can be described as having two parts. The first part is related to the means of  $\alpha_m$  and  $\beta_m$  in Equation (40), and produces a nonrandom distortion which has a peak at the Doppler frequencies of the target and false target. To show this effect,

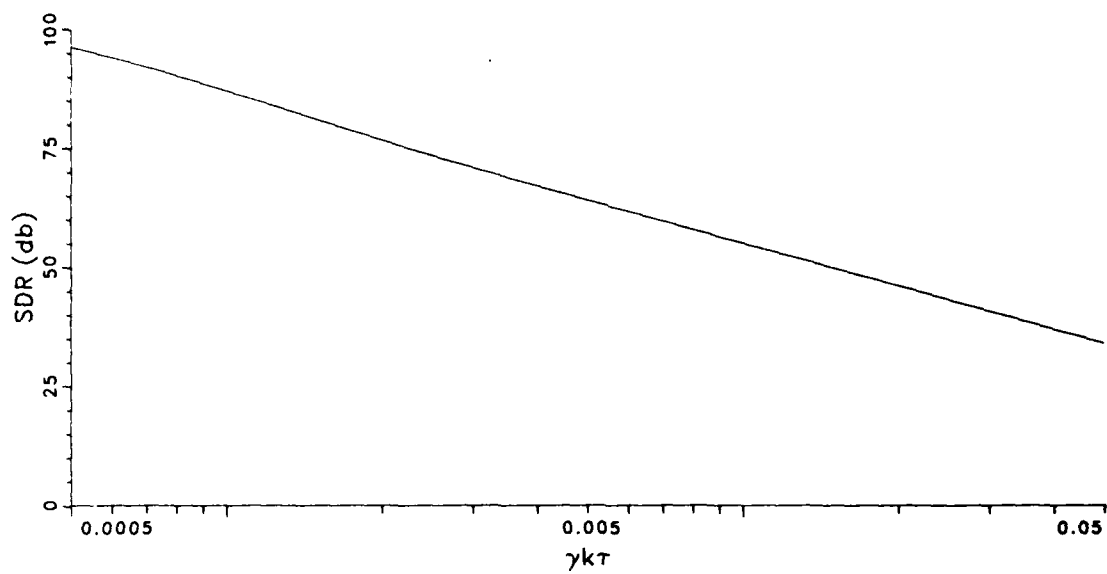


Figure 9. Distortion Level for Independent Random Jitter

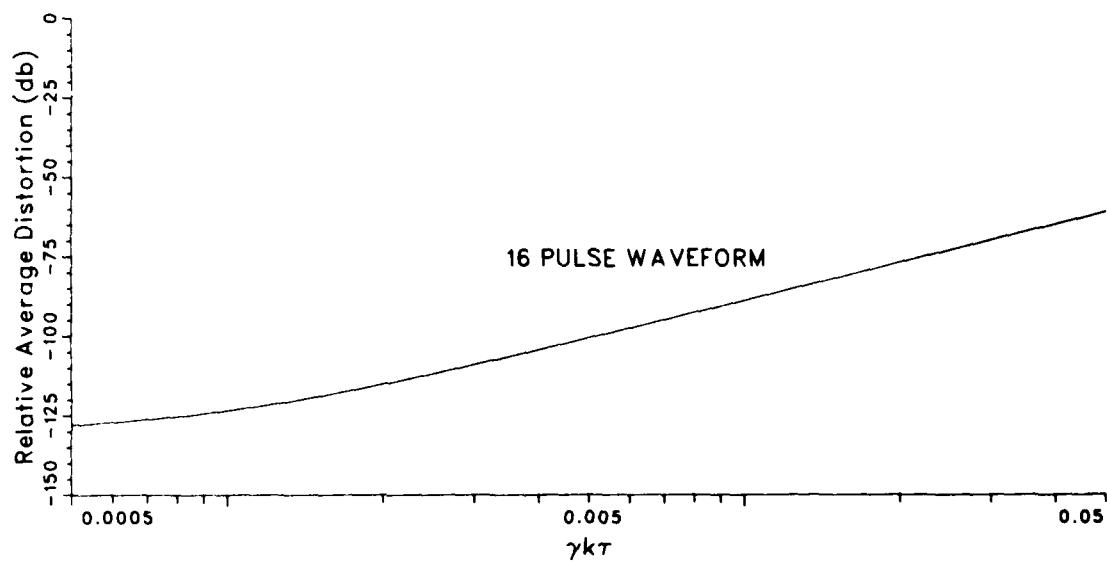


Figure 10. Relative Average Distortion at Doppler Peak

let  $\bar{\alpha}$  and  $\bar{\beta}$  be the means of  $\alpha_m$  and  $\beta_m$  defined in Equation 40. Then, from Equation (24), the jitter-dependent portion of the samples which results from the means of  $\alpha_m$  and  $\beta_m$  is

$$a\bar{\alpha} \cos(2\pi f_m T + \theta) + jb\bar{\beta} \sin(2\pi f_m T + \theta) \quad (44)$$

which appears as samples of sinusoids at the Doppler shifts of the true target and the false target. In the absence of gain and delay mismatch, we have  $a\bar{\alpha} = b\bar{\beta}$  and Equation (44) only contributes at the Doppler shift of the true target. Thus, the distortion is not spectrally flat.

The effect of this first part is shown in Figure 10 which shows the distortion power at the target Doppler shift relative to the corresponding signal power as a function of  $\gamma$ . In this example, we assume a 16 pulse waveform, bandwidth  $k\tau$  much greater than Doppler shift  $f$ , pulse length  $\tau$  much greater than the sampling period  $1/k\tau$ , and no gain or delay mismatch. It is also assumed that that  $r_m$  and  $s_m$  are Gaussian with zero mean and variance  $\gamma^2$ .

The second part of the distortion in the Doppler processor output appears as zero mean complex random variables. Subtracting Equation (44) from the samples in Equation (24) gives the following jitter-dependent component of the samples,

$$a(\alpha_m - \bar{\alpha})\cos(2\pi f_m T + \theta) + jb(\beta_m - \bar{\beta})\sin(2\pi f_m T + \theta) \quad (45)$$

The details are not presented here, but it can be shown that the DFT of Equation (45) leads to zero mean complex Gaussian random variables, with

unequal variances for the real and imaginary parts. The derivation relies on the independence of the  $r_m$  and  $s_m$ , and applies the Lindeberg condition [2] of the central limit theorem in evaluating the real and imaginary components of the DFT outputs. This result is valid even when the DFT inputs are weighted to reduce Doppler sidelobes.

#### 4.3 Combined Jitter Model

The choice of which jitter model to use depends strongly on radar system parameters (e.g., bandwidth, pulse spacing, number of pulses) and on hardware implementation parameters,  $\gamma^2$  and  $\sigma^2$ . When the product  $NT$  is large, the clock frequency stability approach (Section 4.1) becomes more important than the independent random jitter approach (Section 4.2). However, when  $NT$  is small, clock frequency stability is less important than the independent random jitter which is always present.

In those cases where neither jitter model is clearly dominant, the I and Q timing jitter,  $r_m$  and  $s_m$ , may be described as being Gaussian with zero mean and variance  $\sigma^2 \cdot |m-(N-1)/2|$ . This probability density may be used in computing the second moments of  $\alpha_m$  and  $\beta_m$  in Equation (27) which are then used to compute the distortion. The results lead to a distortion formula in a straightforward manner; the derivation is not presented here. The result is interesting, in that the combined distortion,  $D$ , is the sum of  $D_1$  and  $D_2$  plus a cross term. In the case of no gain or delay mismatch,

$$D = D_1 + D_2 + \frac{3}{2} a^2 g_2^2 \gamma^2 \sigma^2 N^2 \quad (46)$$

where the Taylor series approach is used again, and  $D_1$  and  $D_2$  are described by Equations (34) and (42). When mismatch is present, we have the bound

$$D \leq B_1 + B_2 + \frac{3}{2} \gamma^2 \sigma^2 N^2 (a^2 g_2^2 + b^2 g_1^2) \quad (47)$$

where  $B_1$  and  $B_2$  are the bounds defined for  $D_1$  and  $D_2$  in Equations (35) and (43). In both cases, the contribution of the cross terms is small.

## 5. CONCLUSION

The previous sections in this report present an analysis of the effects of I and Q gain mismatch, I and Q timing mismatch, and timing jitter in the sampler of pulse-Doppler radars. The simplest case is gain mismatch which causes a false target to appear at the same range as the true target, but with the opposite Doppler shift. Gain mismatch also causes an SNR loss. Sample timing mismatch causes similar effects to that of gain mismatch, except that the extent of the effects depends on target range and Doppler shift. Timing jitter is somewhat different from the mismatch cases; the result is a distortion in the Doppler processor output and depends on target range and Doppler shift. Timing jitter does not cause a false target to appear unless gain or timing mismatch is present. The distortion gives a signal-to-distortion ratio which, for system clock frequency jitter, is inversely proportional to the square of the burst waveform length. In the case of independent random jitter, the distortion has a spectral peak at the Doppler shift of the target.

### Acknowledgements

The author extends his thanks to Susan J. Andrews for preparing the manuscript of this report, and to Stephen J. Herschkorn for preparing the figures and computer simulations.

### References

- [1] Nathanson, F. E., Radar Design Principles, McGraw-Hill, New York, 1969.
- [2] Feller, W., An Introduction to Probability Theory and its Applications,  
Vol. II, John Wiley & Sons, New York, 1971.
- [3] Apostol, T. M., Calculus, Vol. I, Blaisdell Pub. Co., Waltham, MA, 1969.



## Appendix A

In this approach, it is shown that the mismatch term,  $\delta$ , can be neglected in the sine and cosine arguments in Equation (16), and that similarly the distortion terms,  $r_m \pm \delta$ , can be neglected in the sine and cosine arguments in Equation (22). These simplifications make the analysis in the report considerably easier.

Equation (16) is repeated in Equation (A.1) for convenience,

$$\begin{aligned} x_m = & \cos[2\pi f(mT + \delta) + \theta] G(t' - f/k + \delta, f) \\ & + j \sin[2\pi f(mT + \delta) + \theta] G(t' - f/k - \delta, f) \\ & + n_I(m) + j n_Q(m) \end{aligned} \quad (A.1)$$

In this case,  $\delta$  is a sampling time mismatch and it is very reasonable to restrict the mismatch to be less than one sampling period,  $\delta < 1/k\tau$ .

From the definition of  $G(t, f)$  in Equation (7), the real part of the signal portion of Equation (A.1) can be written as

$$\frac{\cos[2\pi f(mT + \delta) + \theta] \sin[\pi k(t' + \delta)(\tau - |t' - f/k + \delta|)]}{\pi k(t' + \delta)\tau} \quad (A.2)$$

In examining Equation (A.2), it should be noted that, in pulse-Doppler radars, the Doppler shift,  $f$ , should be much less than the bandwidth,  $k\tau$ . Using this relationship and the restrictions on  $t'$  and  $\delta$ , the  $\delta$  component to the argument of the sine in Equation (A.2) is

$$\pi k \delta (\tau - |t' - f/k + \delta|) \approx \pi k \tau \delta \quad (A.3)$$

The  $\delta$  component of the argument to the cosine in Equation (A.2), however, is

$$2\pi f\delta \quad . \quad (A.4)$$

We can now state the relationship between these arguments as

$$2\pi f\delta \ll 2\pi k\tau\delta < \pi \quad . \quad (A.5)$$

Since the  $\delta$  component of the argument to the cosine is much less than that of the sine in Equation (A.2) and also much less than  $\pi$ , it is clear that omitting  $2\pi f\delta$  in the cosine argument in Equation (A.2) will not significantly affect the analysis of the signal. Similarly, the  $2\pi f\delta$  term can be dropped from the sine argument in Equation (A.1) giving the desired result.

The justification for dropping the term  $\pi f(r_m \pm \delta)$  from the sine and cosine arguments in Equation (22) is essentially the same as the discussion for Equation (16) given above. The main difference is that the sampling time jitter plus mismatch should be less than one sampling period so that

$$|r_m \pm \delta| < 1/k\tau.$$

## UNCLASSIFIED

SECURITY CLASSIFICATION OF THIS PAGE (When Data Entered)

REPORT DOCUMENTATION PAGE		READ INSTRUCTIONS BEFORE COMPLETING FORM
1. REPORT NUMBER ESD-TR-83-042	2. GOVT ACCESSION NO.	3. RECIPIENT'S CATALOG NUMBER
4. TITLE (and Subtitle)  Sampling Mismatch and Timing Jitter in Pulse-Doppler Radar		5. TYPE OF REPORT & PERIOD COVERED  Technical Report
		6. PERFORMING ORG. REPORT NUMBER Technical Report 646
7. AUTHOR(s)  Stephen C. Pohlig		8. CONTRACT OR GRANT NUMBER(s)  F19628-80-C-0002
9. PERFORMING ORGANIZATION NAME AND ADDRESS Lincoln Laboratory, M.I.T. P.O. Box 73 Lexington, MA 02173-0073		10. PROGRAM ELEMENT, PROJECT, TASK AREA & WORK UNIT NUMBERS Program Element Nos. 63304A and 63308A
11. CONTROLLING OFFICE NAME AND ADDRESS Ballistic Missile Defense Program Office Department of the Army 5001 Eisenhower Avenue Alexandria, VA 22333		12. REPORT DATE 9 September 1983
		13. NUMBER OF PAGES 44
14. MONITORING AGENCY NAME & ADDRESS (if different from Controlling Office)  Electronic Systems Division Hanscom AFB, MA 01731		15. SECURITY CLASS. (of this report)  Unclassified
		15a. DECLASSIFICATION DOWNGRADING SCHEDULE
16. DISTRIBUTION STATEMENT (of this Report)  Approved for public release; distribution unlimited.		
17. DISTRIBUTION STATEMENT (of the abstract entered in Block 20, if different from Report)		
18. SUPPLEMENTARY NOTES  None		
19. KEY WORDS (Continue on reverse side if necessary and identify by block number)  sampling jitter radar pulse-Doppler mismatch		
20. ABSTRACT (Continue on reverse side if necessary and identify by block number)  Pulse-Doppler processing is an often used technique for extracting range and Doppler information of targets. Such a system can be described as consisting of three basic components, a pulse compressor, sampler, and Doppler processor. When quadrature detection is used, the gains and timing of the sampled inphase and quadrature components of the pulse compressor output must be matched in order to minimize distortion and noise at the Doppler processor output. In addition, the jitter in the sampling times also causes distortion and noise. This report presents an analysis of these effects and describes the signal degradations due to mismatch and jitter in the sampler.		